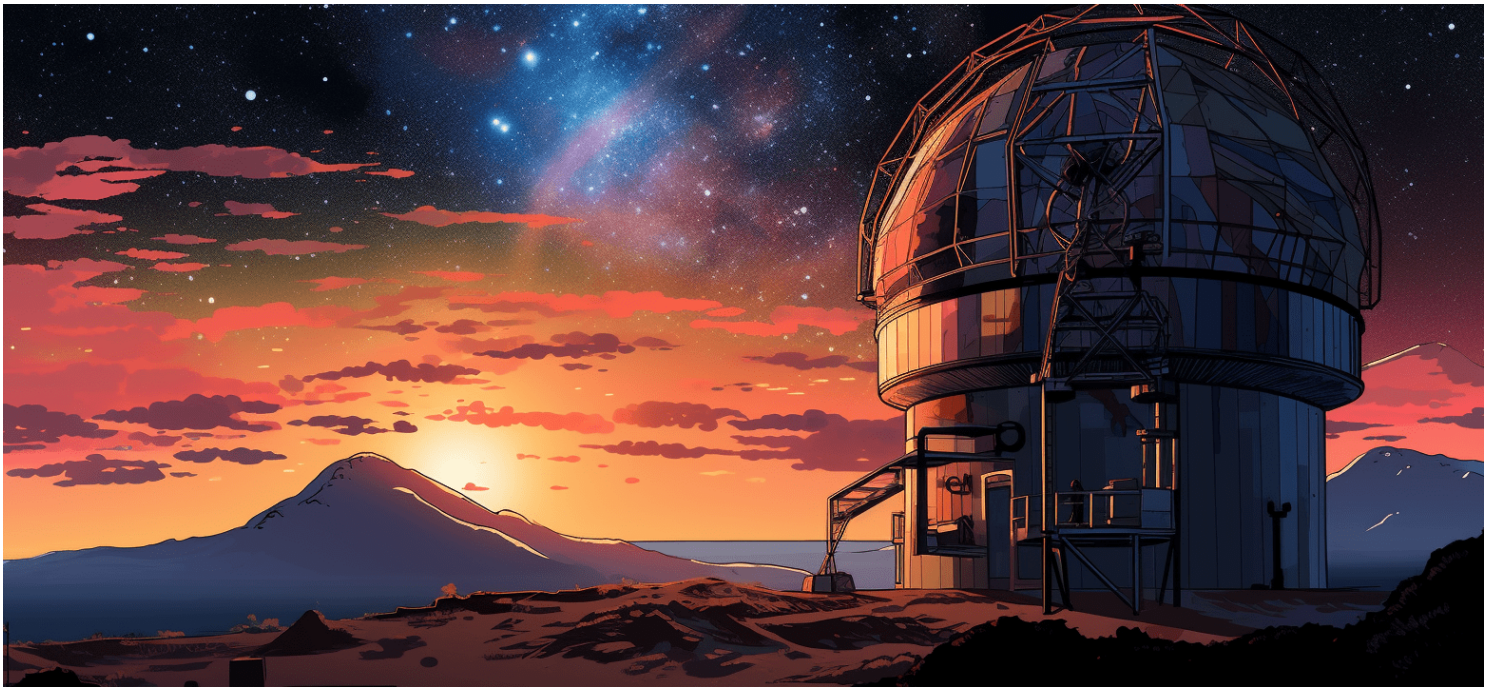




Why Mature Galaxies Seem to have Filled the Universe shortly after the Big Bang

A New Cosmological Model, that Predicted the JWST Observations

Arthur E. Pletcher



v6

Mar 13, 2024

<https://doi.org/10.32388/2X1GDL.6>

Why Mature Galaxies Seem to have Filled the Universe shortly after the Big Bang

A New Cosmological Model, that Predicted the JWST Observations

March 13, 2024

Arthur E. Pletcher¹

¹*International Society for Philosophical Enquiry, Woodbridge, VA, USA*
artpletcher@ultrahighiq.org

Abstract

The Azimuthal Hyper-Projection (AHP) onto spacetime Model of Cosmology is just an extension of the familiar Atlas map of a globe in geography. The Atlas is an azimuthal projection of 3 spacial dimensions projected onto a 2 dimensional plane. The important feature of an Atlas is that the geometry expands asymptotic toward the horizon, and is therefore **positionally dependent**, such that if North America is centrally positioned, then Siberia and Alaska are viewed as extremely remote. Thus if the Bering Strait were centrally positioned, then longitudinal meridians of North America would likewise be viewed as being remotely separated. AHP extends this concept to a hyper-projection of 5 dimensions onto spacetime. However as viewed in spacetime, geodesics appear to be expanding outward in 3 dimensional space away from the observer. Thus by extension, AHP is also **positionally dependent**, such that the separations between remote galaxies appear (measures) to be much greater than they would appear from their mutual local group, and vice versa our local group of galaxies would appear to be mutually separated with extreme distances from a remote perspective. A proposed experiment (figure 14) is offered to prove that two separated objects, as measure from a remote distance ($\sim 40AU$) are greater than their respective distance, as measured locally. Red-shifting is alternatively proposed as azimuthal angular projections of wavelengths λ . Magnitude is alternatively proposed as a function of Lambert's cosine law of illumination, over expanding geodesics. From established z values, the Universal hypersphere is calculated (figure 9). A function of this projected hypersphere is shown to match the Universal expansion rate, as established from supernova cosmology survey points, and also satisfies the Cosmological Constant Λ , without dark energy. Flattened galaxy rotation curves are simply and accurately explained as measured expanding geodesics and apparent increasing density, along the observer's line of sight (figure 11, equation 20). As well, this model provides a reasonable explanation of the James Web Space Telescope findings: of maturely developed galaxies at the time of the early universe. The justification of such a radically novel model is from recent observations from the first dataset, provided by NASA's James Webb Space Telescope (JWST) of six massive galaxies, at a time in the early universe, seem to defy conventional cosmological models, as they appear to be as mature and developed as our own local group. Such unexpected discoveries **justify a radically novel model of Cosmology**. To quote Joel Leja, assistant professor of astronomy and astrophysics at Penn State "It turns out we found something so unexpected it actually creates problems for science. It calls the whole picture of early galaxy formation into question".

Keywords dark matter · Hubble tension · galaxy rotation curve · accelerated universal expansion

1 Introduction

This novel conceptual model upends the cosmological timeline, red-shifting, and accelerating universal expansion. This article begins by describing how global meridians, which are azimuthally projected onto a flat surface, are asymptotic along the surface, toward the horizon (away from the observer), in the familiar "Atlas" (gnomonic projected) mapping. By extension, the hyper-meridians of a \mathbb{R}^4 (four spatial) dimensional hypersphere, azimuthally projected onto a \mathbb{R}^3 (three spatial) dimensional sphere, are shown to be asymptotic along the spherical surface and also away from the observer. A coordinate system is presented (in a cross section) to equate red-shifting of wavelengths λ with azimuthal angular projections, Using this equation, red-shift (z) is revised from: $z = \frac{\lambda_{obs} - \lambda_{rest}}{\lambda_{rest}}$ to be a function of distance x_n and hyperspere arc length (radian) $z = \frac{\lambda \frac{x_n}{a} - \lambda}{\lambda}$. In conjunction with observed red-shifting survey data and Lambert's cosine law of luminous intensity, the universal hyperspere radius is estimated. From these established parameters, it is shown how both velocity and energy density appear to increase along azimuthally projected (skewed) length (x). As well, how galaxies appear to be dilated (or elongated), along the line of sight, with a resulting flattened rotation curve. From these established parameters, a function is developed to plot a curve, which is superimposed upon graphs (Distance modulus (μ) vs red-shift (z)) of data points from the HST Key Project. discrepancies between theoretical and observed galaxy rotation curves, as well as apparent increased energy density are shown to be predicted from this model.

2 Intuition of the Azimuthal Hyper-Projection Model of Cosmology

The familiar Atlas map, which is an \mathbb{R}^2 azimuthal global projection, typically places Siberia and Alaska at opposite extremes. However, they are locally connected at the Bering Strait, as viewed in \mathbb{R}^3 space. See figure 1.

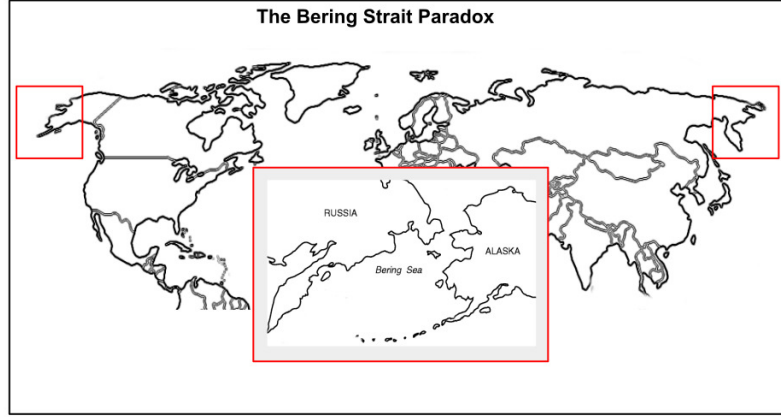


Figure 1: Atlas map, which is an \mathbb{R}^2 azimuthal global projection

The Azimuthal Hyper-Projection Model of Cosmology proposes the following hypothesis:

Hypothesis 1 (H1) *As an Azimuthal Hyper-Projection onto spacetime is asymptotic to an outward horizon, the geometric perspective is based to the position of the observer, such that all projected geodesics will appear to be expanded outwardly, from the arbitrary biased perspective of the observer. This effect is similar to the familiar atlas map, which when viewed from North America, typically places Siberia and Alaska at opposite extremes. Therefore, the apparent distances between remote galaxies could actually be local neighbors, and vice versa, from their perspective.*

Azimuthal Projections onto an \mathbb{R}^2 Plane Appear to Expand Outward from the Observer, along the plane

Figure 2 shows an observer on a \mathbb{R}^2 plane, positioned along a tangent of a \mathbb{R}^3 sphere, measures projected meridians at distance x_n , per the equation [1]:

$$x_n = R \tan(\theta) \quad (1)$$

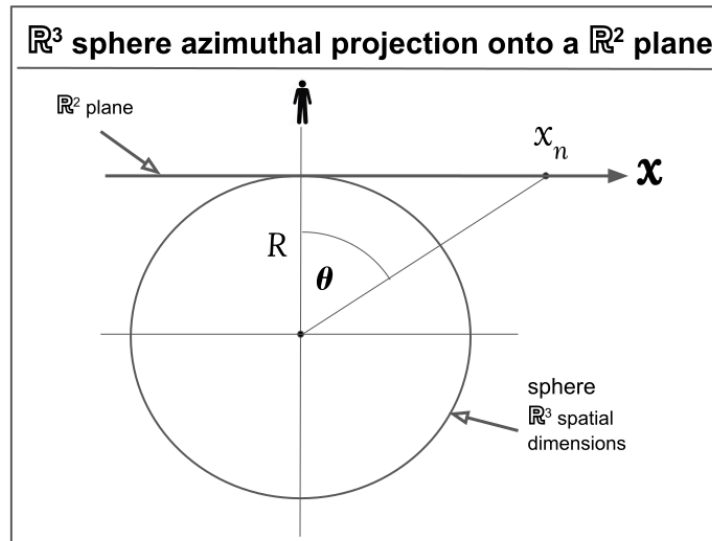


Figure 2: \mathbb{R}^3 sphere azimuthally projected onto a \mathbb{R}^2 plane. Distance from angle θ and radius of sphere.

Figure 3 shows how azimuthally projected meridians are asymptotic along the \mathbb{R}^2 plane, and toward the horizon (away from the observer).

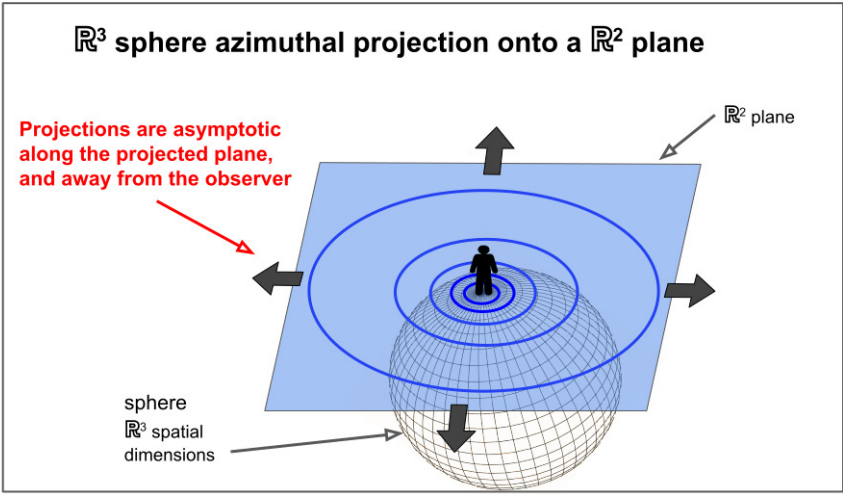


Figure 3: meridians are asymptotic along the \mathbb{R}^2 plane, and toward the horizon (away from the observer).

Figure 4 shows how azimuthal projections expansion is relative to the observer's position. On the left side, the observer is positioned along a tangent at projection a , and expansion increases toward point g . However on the right side, the observer is positioned along a tangent at projection g , and expansion increases toward point a .

Positional Dependence of Projection Expansion

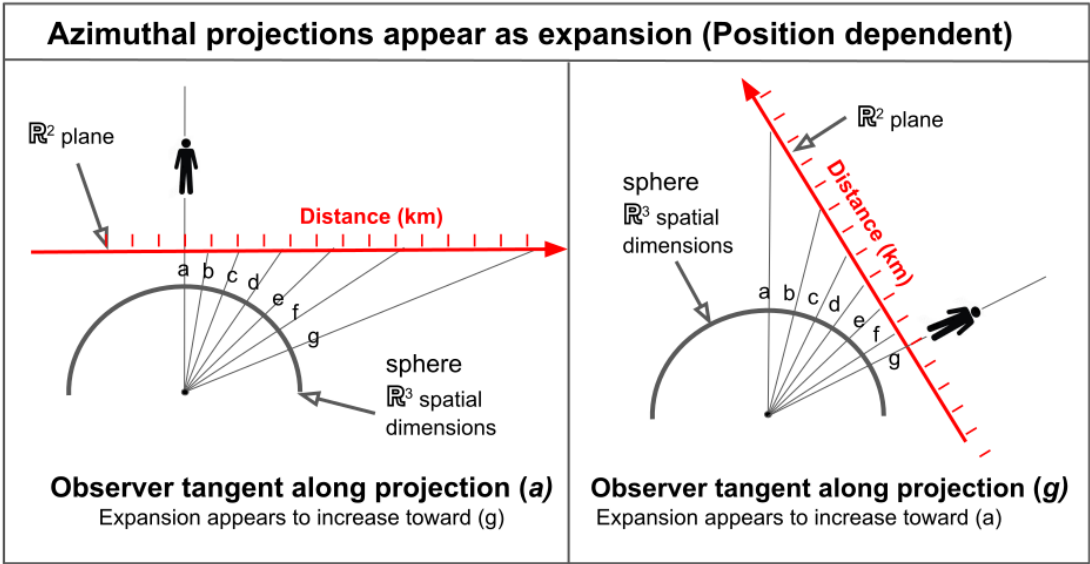


Figure 4: Azimuthal projections appear as expansion (Position dependent)

3 \mathbb{R}^4 Hypersphere Azimuthal Projections onto an \mathbb{R}^3 Sphere Appear to Expand outward from the Observer in three spacial dimensions

Figure 5 shows how azimuthally projected hyper-meridians are asymptotic along the \mathbb{R}^3 sphere, and outward from the observer.

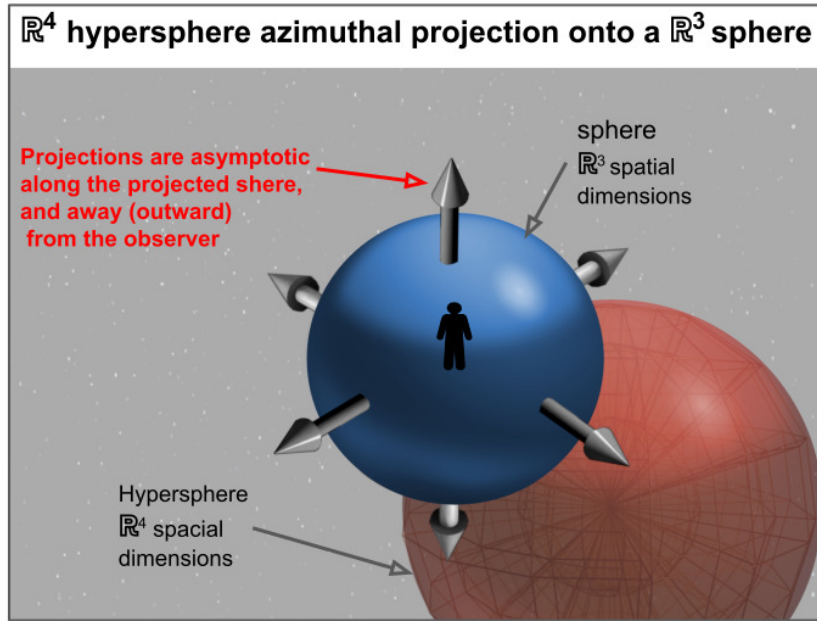


Figure 5: \mathbb{R}^4 hypersphere azimuthally projected onto a \mathbb{R}^3 sphere. hyper-meridians are projected asymptotic along the sphere, and away from the observer.

Figures 6 and 7 show how azimuthal projections red-shifting is relative to the observer's position. On the left side, the observer is positioned along a tangent at projection a , and red-shifting increases toward point g . However on the right side, the observer is positioned along a tangent at projection g , and red-shifting increases toward point a . A radical implication of this model is that azimuthal angular projections are positional dependent, thus degrees of redshifting over distance is positional dependent. It's conceivable that our local group would appear to be much more expanded, from the perspective of remote observer, and vice versa; vastly remote galaxies would appear to spaced much closer together, from the perspective of a remote observer.

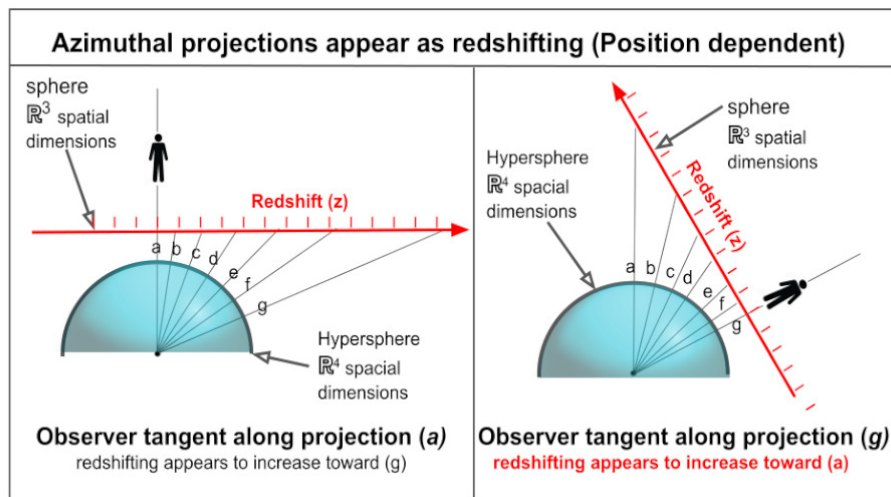


Figure 6: Azimuthal projections appear as red-shifting (Position dependent)

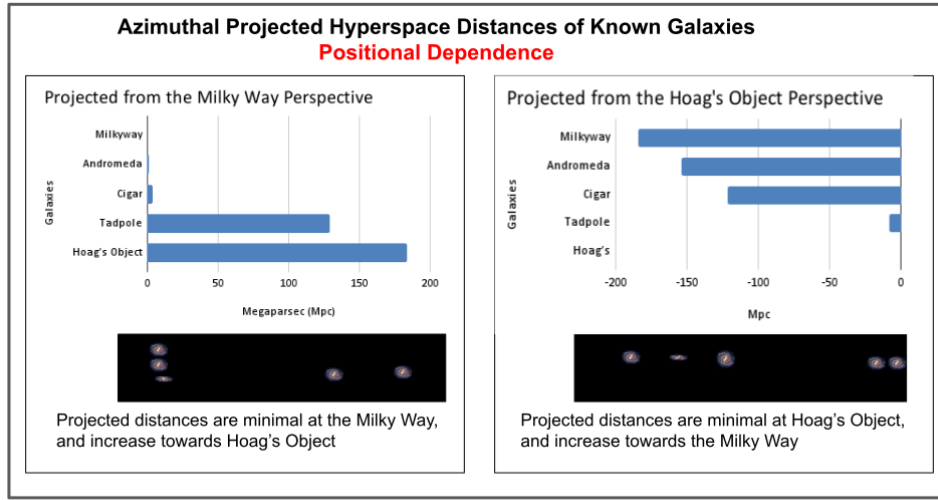


Figure 7: Positional Dependence of known Galaxies

4 Red-shifting is Alternatively Proposed as Azimuthal Angular Projections of Wave-lengths λ

As Azimuthal projections are asymptotic along the observer's line of sight, obliqueness increases with distance x . Thus wave lengths become stretched along the observer's line of sight x . The observer in spacetime can not directly observe the projections in hyperspace, and is limited to his line of sight on the x direction. Figure 8 shows how the observer measures the wave lengths λ to be skewed (red-shifted). Section $B - B$, the "at rest" wavelength λ_{rest} , is normal to the hyperspheric surface. Oblique view $A - A$ is the "observed" wavelength λ_{obs} , with a skewed (elongated) wavelength.

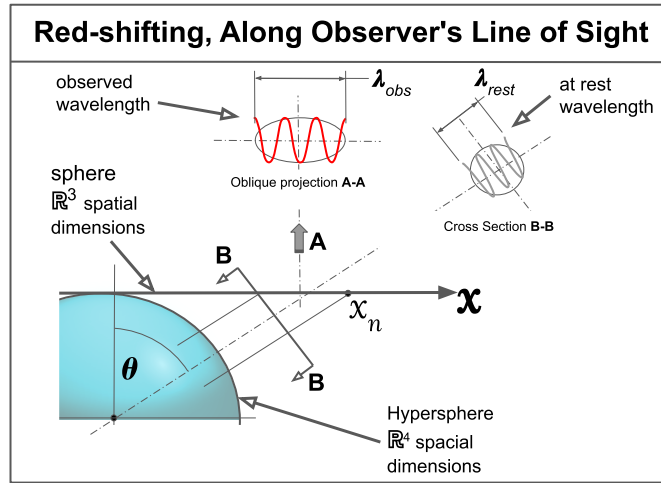


Figure 8: Red-shifting, Along Observer's Line of Sight.

5 Revised Formula for Red-shiff (z)

Figure 9 is a 2 dimensional cross section of an \mathbb{R}^4 (spatial dimensions) hypersphere Azimuthal projected onto a \mathbb{R}^3 (spatial dimensions) sphere, and extended along X axis into macrospace. A classic space observer resides along the X axis at reference frame: $x = 0$, from which all measurements ($x_n \neq 0$) are skewed projections, asymptotic to the horizon.

$$S \in \mathbb{R}^2 \text{ def } = (x, y) || \sqrt{x^2 + y^2} = r || \quad (2)$$

$$F : S \rightarrow / (x) [0, x_n] \quad (3)$$

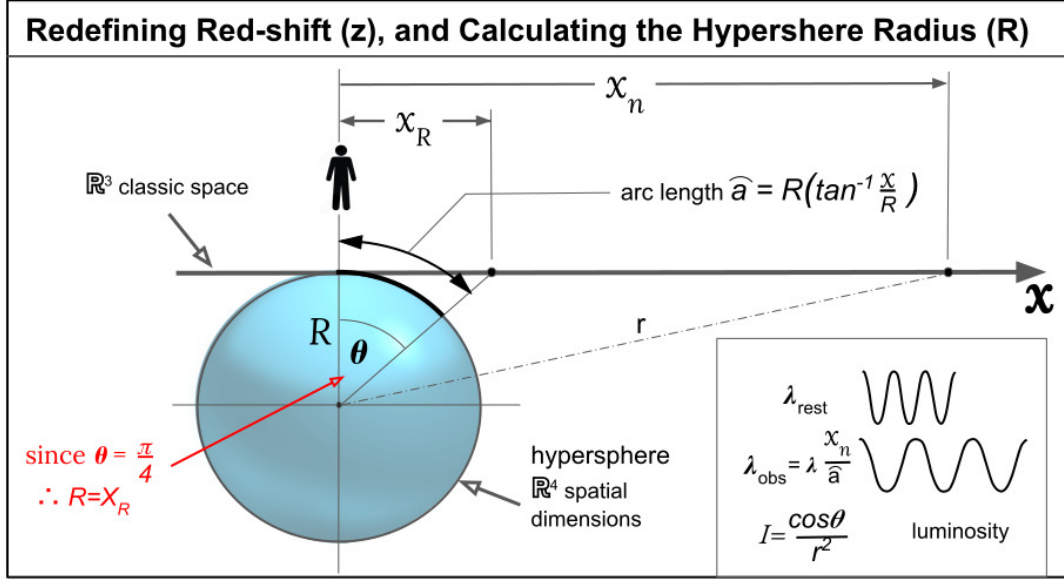


Figure 9: Revised redshift (z), and radius of hypershere

Hyper-meridians and celestial bodies are Azimuthally projected as lateral straight lines, per equation 5:

$$x_n = R \tan \theta$$

Solving for R :

$$R = \frac{x_n}{\tan \theta} \quad (4)$$

$$\widehat{a} = R \theta \implies \quad (5)$$

$$\widehat{a} = R \left(\arctan \frac{x_n}{R} \right) \quad (6)$$

Framed within this model, electromagnetic wavelengths of λ , along the hypersphere circumference of radius R , are considered to be at rest. However, x_n is projected (skewed) along the X axis and observed with resulting redshift (z), similar to the redshifting equation [2]:

$$z = \frac{\lambda_{obs} - \lambda_{rest}}{\lambda_{rest}} \quad (7)$$

In this alternative model, $\lambda_{obs} = \lambda \frac{x_n}{\widehat{a}}$,

$$z = \frac{\lambda \frac{x_n}{\widehat{a}} - \lambda}{\lambda} \quad (8)$$

Calculating the Universal Hypersphere Radius

The radius R of the hypersphere can be deduced from a spacetime perspective (Where humans reside), by considering, that observed **distance** (x_R) **must be equal to radius R when the \tan of θ is equal to 1, or when $\theta = \frac{\pi}{4}$** . Thus from the z value, where

$\widehat{a} = R\frac{\pi}{4}$, and $x_R = R$, radius R is derived,

$$\widehat{a} = R\left(\frac{\pi}{4}\right) \quad \text{Substituting } \frac{\pi}{4} \text{ for } \theta \text{ in equation 5} \quad (9)$$

$$z = \frac{\lambda\left(\frac{x_n}{R\frac{\pi}{4}}\right) - \lambda}{\lambda} \quad \text{Inserting into equation 8} \quad (10)$$

$$z = \frac{x_n}{R\left(\frac{\pi}{4}\right)} - 1 \quad \text{cancelling } \lambda \quad (11)$$

$$z = \frac{R}{R\left(\frac{\pi}{4}\right)} - 1 \quad \text{Since } x_n = R, \quad (12)$$

$$z = \left(\frac{4}{\pi}\right) - 1 \quad \text{Simplifies to,} \quad (13)$$

$$z = 0.273 \quad (14)$$

Finding R from $z = 0.273$, using the approximate distance formula,

$$d \approx \frac{zc}{H_0} \quad (15)$$

At current H_0 value of: 73.8 km/sec/Mpc

$$R \approx \frac{0.273 * 299792 \text{ km/sec}}{73.8 \text{ km/sec/Mpc}} \Rightarrow \quad (16)$$

Thus, the radius of the \mathbb{R}^5 hypersphere,

$$R \approx 1108.987 \text{ Mpc} \quad (17)$$

6 Accelerated Universal Expansion is Alternatively Proposed, as \mathbb{R}^5 Azimuthal Projections of Meridians, Asymptotical to a Horizon, and Lambert's Cosine law of Luminous Intensity

Velocity Appears to Increase Along Projected Length x_n

In figure 9. Light-waves and energy density are constant along arc length \widehat{a} . However,

Theorem 1 As \mathbb{R}^5 hyper-spacetime is azimuthal projected onto \mathbb{R}^4 spacetime, From the r.f. of an observer on the projected surface, topology is skewed (elongated), and appears expanded outward from the observer. As a result, celestial bodies appear to be traveling along expanded projected geodesics with increasing velocities (v). This apparent increase of velocity is equivalent to a decreased time interval ($-\Delta t$). Light-waves appear to travel along X_n with an increased velocity \vec{v}' of:

$$\frac{\vec{v}'}{\vec{v}} = \frac{X_n}{\widehat{a}} \quad (18)$$

Calculating z per Distance x

Now that R (The radius of the hypersphere) has been established, values of z can be determined from any value of x_n . Note that x_n is a one dimensional cross-section of the space which humans measure galactic distance, although it is actually a skewed projection of hyper-arc length \widehat{a} onto classic space. Thus, from values of distance modulus μ and established radius R , theta is easily determined. Subsequently from theta, \widehat{a} is determined. Finally from equation 8, z is derived at any distance x_n .

Energy Density Increases along Length X_n

Corollary 1.1 As velocity along skewed x appears to increase per equation 18, energy density ρ proportionally increases, due to increased velocities in particle kinetic and internal energies (compression, energy of nuclear binding, etc.). The observer at $x = 0$ measures volume at x_n [mpc] with increased energy density ρ_n per equation:

$$\frac{\Delta\rho_n}{\Delta\rho} = \frac{(x_n - R)}{R}$$

Lambert's Cosine Law of Illumination

Consider that figure 9 describes an oblique projection of a source S with an illuminate value I . According to Lambert's Cosine Law of illumination [3], intrinsic values of such projected light will decrease in value with θ per equation:

$$I = \frac{\cos \theta}{r^2} \quad (19)$$

In this model, the luminous intensity of type Ia supernovae would decrease, accordingly. Thus, conventionally accepted standard candle measurements along x , would need to be recalculated per Lambert's Cosine Law.

7 Galaxy Rotation Curve with Increased Density

The discrepancies between theoretical and observed galaxy rotation curves involve both density and velocity. Conventionally, the dependence of circular velocity V_{circ} on radial distance R assumes M , m and velocity to be fixed over large scales in Kepler's law, [4]

$$T^2 = \frac{4\pi^2 r^3}{GM} \Rightarrow T^2 \propto r^3$$

Moreover, gravitational lensing demonstrates the existence of a much greater Mass (density) than the sum of the stars within the galaxy. **However, this alternate model specifically addresses these two issues and provides an alternative explanation,**

Kepler's Law rearranged as density ρ integrated over time dt

Corollary 1.2 Velocity \tilde{v} and density ρ_n are measured with increased magnitude per distance x_n . This directly extends to energy density within galaxies and the effects on rotational velocity, such that: As x_n increases, centripetal force is perfectly balanced by increases in \tilde{v} and, subsequently, ρ_n ,

$$\frac{v^2}{r} = \frac{G}{r^2} M = \frac{G}{r^2} \int \rho_n dt \quad (20)$$

Note: total mass M inside the circle of the radius r can be obtained by doing integration of mass density in a volume. $M = \int \rho_n dt$. $\rho = \rho_R$ and ρ_M (Dark components are excluded from this model, with the intent of presenting an alternative).

Figure 11 shows how skewed projected meridians, along the observer's line of sight, appear elongated and are measured with greater density. The result is a flattened rotation curve, per $\frac{x}{a}$. Thus, an elongated galaxy appears to have greater rotational velocity, and energy density.

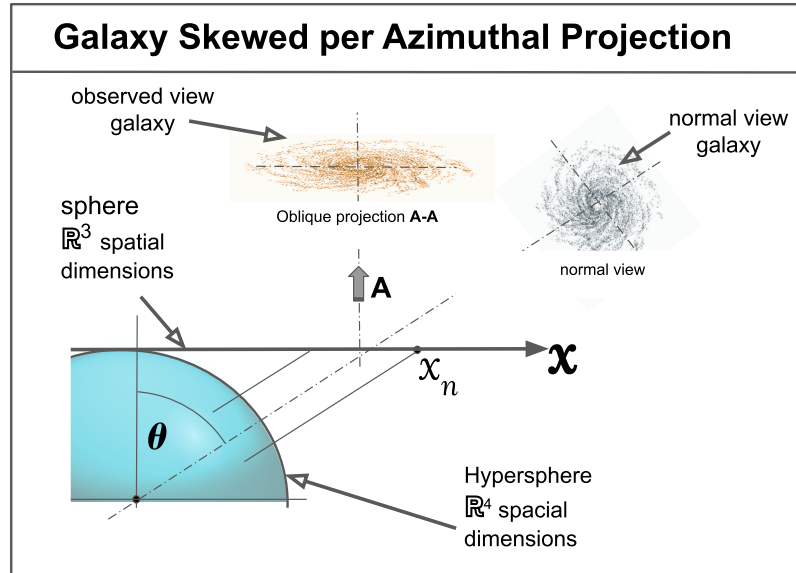


Figure 10: Spiral galaxy projection is skewed

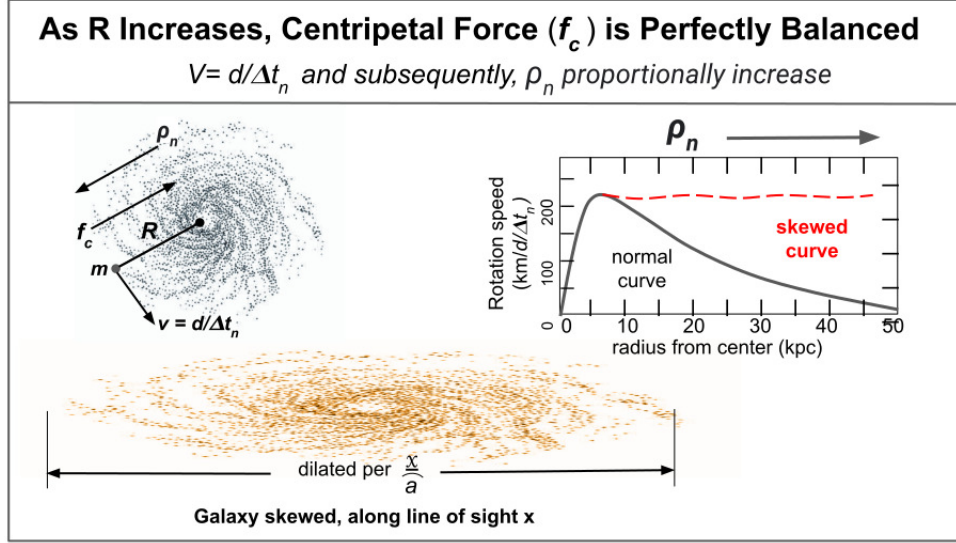


Figure 11: Elongated galaxy appears to have greater rotational velocity, and energy density.

$$\lim_{r \rightarrow -r_n} \frac{\partial \rho}{\partial (ar)} = \lim_{r \rightarrow +r_n} \frac{\partial \rho_n}{\partial (ar)}$$

8 Graphing a Function that conforms with the Hubble Diagram

From this model of higher dimensional gnomonic projection, function $F(z)$ provides a graph to compare with Supernova Cosmology Survey Points. Using z as the dependent variable, and μ as independent variable, such that $F(z)$ is a function of μ . From x_n in equation 7, Using equation 6, and converting R to mega parsecs.

$$\lambda X_n = \left(\lambda_{rest} \frac{x}{1108.987 \left(\arctan \frac{x}{1108.987} \right)} \right) \quad (21)$$

Inserting into equation 7,

$$z = \left[\frac{\left(\lambda_{rest} \frac{x}{1108.987 \left(\arctan \frac{x}{1108.987} \right)} \right) - \lambda_{rest}}{\lambda_{rest}} \right] \quad (22)$$

λ_{rest} cancels, leaving,

$$z = \left[\left(\frac{x}{1108.987 \left(\arctan \frac{x}{1108.987} \right)} \right) \right] - 1 \quad (23)$$

Converting redshift z to velocity km/sec ,

$$F = \left[\left(\frac{x}{1108.987 \left(\arctan \frac{x}{1108.987} \right)} \right) - 1 \right] * 300,000 km/sec \quad (24)$$

Substituting Lambert's equation (19) for x ,

$$F = \left[\left(\frac{x(1108.987 * \cos(\arctan(\frac{x}{1108.987})))}{\left(\frac{\cos(\arctan(\frac{x}{1108.987}))}{x^2 + 1108.987^2} \right)^2 + 1108.987^2} \right) - 1 \right] * cK \quad (25)$$

Where K is a slope correction constant, which is necessary to offset conventional measurements of standard candle distances.

Table 1 lists extrapolated points, at $50(Mpc)$ intervals, of Function $F : d \mapsto v \mid F = \{v, f(d)\} [0.000, 5 \times 10^8]$. Also, corresponding values of μ and z

Figure 12 shows the Function $F : d \mapsto v \mid F = \{v, f(d)\} [0.000, 5 \times 10^8]$

Table 1: Extrapolated points of function F . In successive columns: [pc] (distance parsec), [km/s] (kilometers per second), [μ] (Distance modulus), [z] (redshift),

pc	km/s	μ	z
5.000E+07	4.129E+03	33.495	0.014
1.000E+08	8.228E+03	35.000	0.027
1.500E+08	1.227E+04	35.880	0.041
2.000E+08	1.622E+04	36.505	0.054
2.500E+08	2.006E+04	36.990	0.067
3.000E+08	2.377E+04	37.386	0.079
3.500E+08	2.734E+04	37.720	0.091
4.000E+08	3.074E+04	38.010	0.103
4.500E+08	3.397E+04	38.266	0.113
5.000E+08	3.703E+04	38.495	0.124

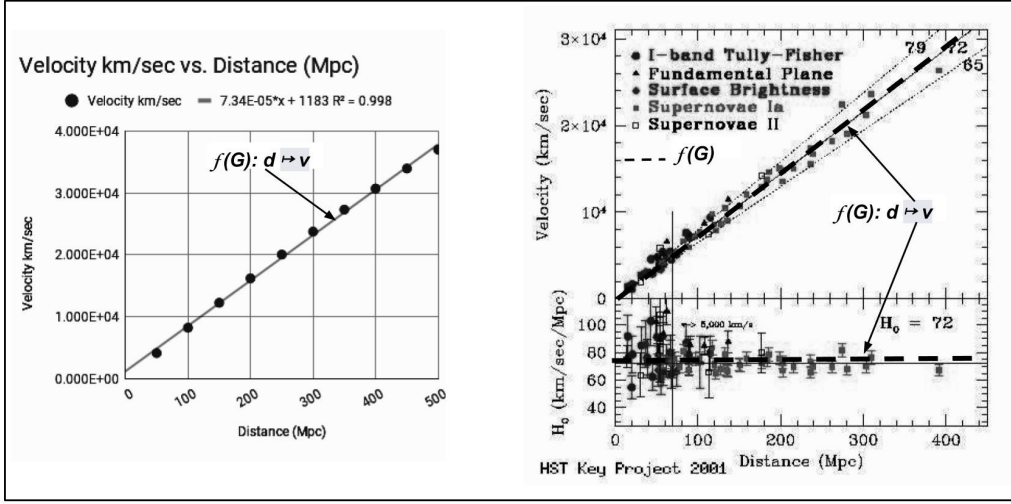


Figure 12: Left: Function $F : d \mapsto v$, with extrapolated points. Right: Function F superimposed onto the HST Key Project

Figure 13 shows the Function $F : z \mapsto \mu \mid F = \{\mu, f(z)\} [0.000, 0.125]$. **Note the familiar curve (in logarithmic scale), which is conventionally interpreted as "accelerated expansion".**

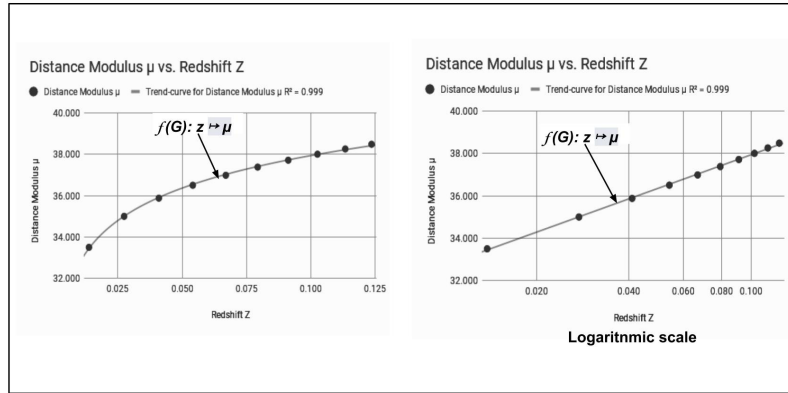


Figure 13: Left: Function $F : z \mapsto \mu$, with extrapolated points. Right: Function F with logarithmic scale, along z axis. **Note the familiar curve, which is conventionally interpreted as "accelerated expansion".**

9 Experiment to prove a 5th Dimension Azimuthal Projection, Using Laser Ranging

Figure 14 Describes an experiment using lazer ranging and reflectors, to provide proof of a projected 5th Dimension in Cosmol-ogy:

Reflectors $R1$ and $R2$ are positioned at a great distance from Earth ($40AU$) in the outer solar system, with a lesser distance between the two reflectors ($5AU$). Proof would be: If the distance between reflectors $R2$ and $R1$, as measured from Earth, is greater than the distance between reflectors $R2$ and $R1$, as measured remotely from $R2$. ($R2_E - R1_E$) > ($R2_r - R1_r$)

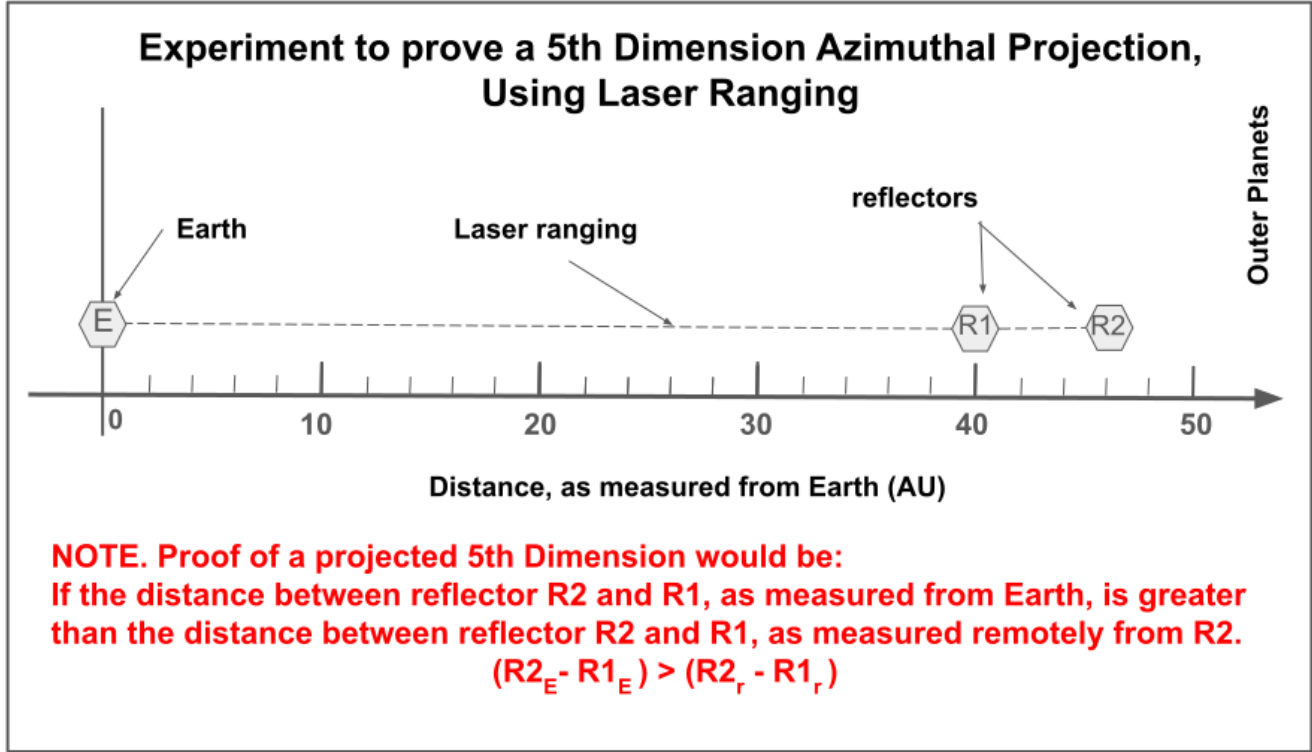


Figure 14: Experiment to prove a 5th Dimension Azimuthal Projection, Using Laser Ranging

10 Supportive Evidence of the \mathbb{R}^5 Azimuthal Projection Model

Galaxy Recession velocities (z red-shift and blue-shift) will be measured greater on the far side of galaxies. Such a closed system expanding in azimuthal projected hyperspace **would defy the standard model of accelerated universal expansion and dark energy**, where only space between galaxies are assumed to be expanding. Theorem 1, is supported by the following correlation study[5] "On Possible Systematic Redshifts Across the Disks of Galaxies" . This study shows a deviation from Kepler's orbital laws, specifically on the subject of increased velocity on the far sides of multiple galaxies. Although not conclusive, it does justify consideration to this article.

Note that multiple galaxy surveys with increased velocities across their minor axis. Thus, **velocity within the same body appears to increase per distance**. "Velocity observations in 25 galaxies have been examined for possible systematic redshifts across their disks: a possible origin for the redshifts could be the radiation fields. Velocities increase towards the far sides in most cases. This is so for the ionized gas, for neutral hydrogen, and in some cases for the stars. The effect is seen as velocity gradients along the minor axes, as well as in velocity fields of neutral hydrogen in other parts of the galaxies. Deviation of the kinematic major axis from the optical axis is found for 10 galaxies and in 9 of these the largest velocities occur in the far side. In the central regions of four galaxies are found large velocity gradients in the same direction. While expanding motions provide an explanation for some of these features, it remains difficult to thereby explain all the peculiarities found. Faintness of the data available in this preliminary study should be noticed. Observations specially programmed for this subject would be necessary."

table 2 lists 25 galaxies, correlation coefficients and relevant columns (including sources of data):

Table 2: List of galaxies for which velocities along the minor axes are available. In successive columns: type; distance; angle between rotation axis of galaxy and line of sight; regression and correlation coefficients between velocity and distance; source of data

NGC	Type	d(Mpc)	i	$h(kms^{-1}kpc^{-1})$	corr	source of data
244	Sb	0.69	77°	0.20	0.272	Gottzman and Davis (1970)
253	Sc	4.0	78	0.13	0.012	Burbridge et al. (1963a)
300	Sd	2.4	43	1.03	0.844	Shobbrook and Robinson (1967)
598	Scd	0.72	57	1.51	0.866	Goordon (1971)
613	SBbc	15	47	57.09	0.820	Burbridge et al. (1964c)
972	SBc	17	66	-11.31	-0.670	Burbridge et al. (1964c)
1084	Sc	14	65	-4.75	-0.338	Burbridge et al. (1965)
1097	SBd	12	50	5.00	-0.105	Burbridge and Burbridge (1960)
1365	SBd	15	66	-79.21	-0.976	Burbridge et al. (1962a)
1792	Sbc	10	64	10.12	-0.578	Rubin et al. (1964)
2403	Scd	3.3	55	0.04	0.118	Burns and Morton (1971)
3310	Sbc	11	31	61.27	0.815	Walker and Chincarini (1967)
3521	Sbc	7.6	66	7.18	0.056	Burbridge et al. (1964b)
4736	Sab	3.3	40	44.28	0.849	Walker and Chincarini (1967)
4826	Sab	7.3	60	39.16	0.854	Rubin et al. (1965)
5194	Sbc	4.0	35	-15.18	-0.758	Burbridge et al. (1964a)
5248	Sbc	11	55	-26.94	-0.690	Burbridge et al. (1962b)
5457	Scd	3.5	27	-1.40	-0.403	Rogstad and Stoshak (1971)
6574	Sba	33	45	4.73	0.428	Demoulin and Tung Chan (1969)
27469	Sa	51	49	8.69	0.552	Burbridge et al. (1963c)

11 Observational Phenomena of the \mathbb{R}^5 Azimuthal Projection Model

The Azimuthal Projection Model implies the following observational phenomena for research and experimentation:

The planets in our solar system will deviate from their Kepler / Newtonian orbits by an increased radius and velocity, as their distance from Earth increases. Figure 15 is exaggerated for clarity.

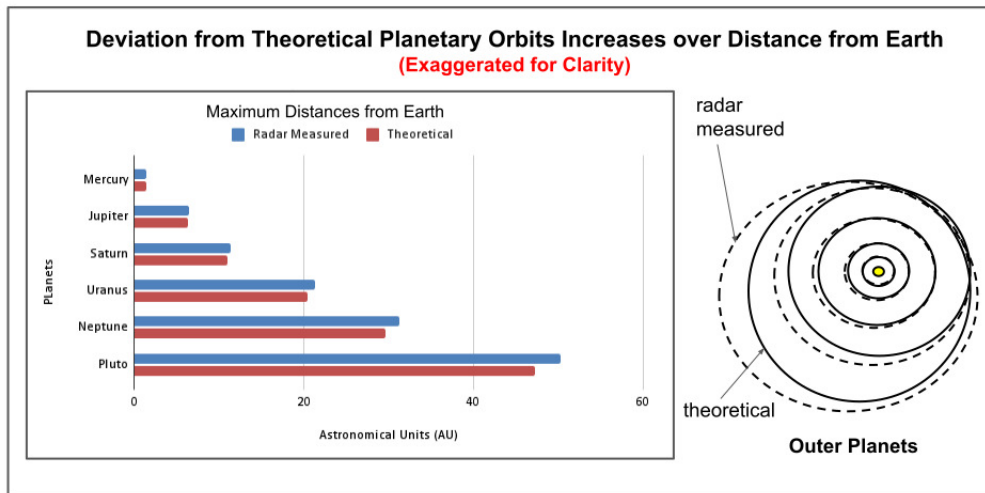


Figure 15: Deviation from Theoretical Planetary Orbits Increases over Distance from Earth

12 Conclusion

This parsimonious model resolves the following mysteries in Cosmology:

- It does not require dark energy to satisfy the Cosmological Constant Λ .
- The JWST findings of mature galaxies at the beginning of the universe.
- Galaxy rotation curves (increased density toward the outer galaxy spin).
- Accelerated universal expansion.
- Note that this model can be experimentally proven (figure 14).

References

- [1] Coxeter H. Introduction to Geometry (2). Wiley, Manhattan, 1969.
- [2] Taylor E and Wheeler JA. Spacetime Physics. WH Freeman and Company, New York, 1992.
- [3] R Waynant. Electro-Optics Handbook. McGraw-Hill, 1994.
- [4] Butikov E. Motions of Celestial Bodies. IOP Publishing, Philadelphia, 2014.
- [5] T. Jaakkola, P. Teerikorpi, and K. Donner. On possible systematic redshift across the disks of galaxies. Astronomy and Astrophysics., 1975.

Data Availability Statement: No Data associated in the manuscript